

Classical radio source propagating into outer HI disc in NGC 3801

B. H. C. Emons^{1*}, C. Burnett^{2,1†}, R. Morganti^{3,4}, C. Struve^{3,4}

¹*CSIRO Astronomy and Space Science, Australia Telescope National Facility, PO Box 76, Epping NSW, 1710, Australia*

²*School of Physics, University of Melbourne, Parkville, Victoria 3010, Australia*

³*Netherlands Institute for Radio Astronomy, Postbus 2, 7990 AA Dwingeloo, the Netherlands*

⁴*Kapteyn Astronomical Institute, University of Groningen, P.O. Box 800, 9700 AV Groningen, the Netherlands*

ABSTRACT

We present observations of a large-scale disc of neutral hydrogen (HI) in the nearby Fanaroff & Riley type-I radio galaxy NGC 3801 with the Westerbork Synthesis Radio Telescope. The HI disc (34 kpc in diameter and with $M_{\text{HI}} = 1.3 \times 10^9 M_{\odot}$) is aligned with the radio jet axis. This makes NGC 3801 an ideal system for investigating the evolution of a small radio source through its host galaxy’s cold ISM. The large-scale HI disc is perpendicular to a known inner CO disc and dust-lane. We argue that the formation history of the large-scale HI disc is in agreement with earlier speculation that NGC 3801 was involved in a past gas-rich galaxy-galaxy merger (although other formation histories are discussed). The fact that NGC 3801 is located in an environment of several HI-rich companions, and shows indications of ongoing interaction with the nearby companion NGC 3802, strengthens this possibility. The large amounts of ambient cold ISM, combined with X-ray results by Croston, Kraft, & Hardcastle (2007) on the presence of over-pressured radio jets and evidence for an obscuring torus, are properties that are generally not, or no longer, associated with more evolved FR-I radio sources. We do show, however, that the HI properties of NGC 3801 are comparable to those of a significant fraction of nearby low-power compact radio sources, suggesting that studies of NGC 3801 may reveal important insight into a more general phase in the evolution of at least a significant fraction of nearby radio galaxies.

Key words: galaxies: active – galaxies: evolution – galaxies: individual: NGC3801 – galaxies: interactions – galaxies: ISM – galaxies: jets

1 INTRODUCTION

Over the past decade it has become clear that radio sources emanating from super-massive black-holes in the centres of galaxies are - rather than merely a by-product of galaxy evolution - key players in the formation and evolution of galaxies throughout the Universe. It is now fairly well established that the properties of Active Galactic Nuclei (AGN) are intimately linked with the properties of their host galaxies. While empirical evidence has established the co-evolution of massive black holes and their host galaxies at various redshifts (e.g. Ferrarese & Merritt 2000, Alexander et al. 2005, see also Silk & Rees 1998), numerical simulations demonstrate that AGN-induced outflows are important feedback processes for clearing the circum-nuclear regions and halting the growth of the super-massive black-holes, regulating the correlations found between the

black-hole mass and the host galaxy’s bulge properties and preventing the formation of too many massive galaxies in the early Universe (e.g. Di Matteo, Springel, & Hernquist 2005, Springel, Di Matteo, & Hernquist 2005, Hopkins et al. 2005, Wagner & Bicknell 2011).

An important phase of AGN feedback is when synchrotron jets emanating from the central black-hole region start propagating into the host galaxy’s inter-stellar medium (ISM). At high redshifts, radio sources are observed to be aligned with optical continuum from warm gas and stars (Chambers, Miley, & van Breugel 1987, McCarthy et al. 1987) and the gas in these regions is characterised by highly disturbed kinematics (McCarthy, Baum, & Spinrad 1996, Villar-Martín, Binette, & Fosbury 1999, Humphrey et al. 2006). This indicates that radio sources vigorously interact with the host galaxy’s ISM, entrain and expel gas and induce or quench star formation (e.g. Bicknell et al. 2000). At intermediate and low redshifts, powerful radio jets are known to induce fast ($> 1000 \text{ km s}^{-1}$) outflows of ionised and neutral gas (e.g. Tadhunter 1991; Clark et al. 1998;

* E-mail:bjorn.emonts@csiro.au

† ATNF Summer Student 2009/10

Oosterloo et al. 2000; Morganti et al. 2003, 2005a,b, 2007; Emonts et al. 2005; Holt et al. 2006, 2008, 2011) and can shock-heat the molecular gas (Guillard et al. 2011), exerting significant feedback on the host galaxy’s ISM.

While propagating radio jets thus have a profound impact on their surrounding ISM, the reverse is also true (see simulations by e.g. Saxton et al. 2002a,b; Jeyakumar et al. 2005; Bicknell & Sutherland 2006; Sutherland & Bicknell 2007). It is well established that external factors, in particular the inter-stellar and inter-galactic medium (ISM and IGM), shape the morphological and physical properties of radio sources. For example, there is strong evidence that radio sources in general show a degree of intrinsic asymmetry (apart from orientation effects), which is most prominent in compact sources (Saikia et al. 1995, 2001, 2003a). Compact radio sources also show a larger degree of polarisation asymmetry than extended sources, suggesting a link between the propagating radio jets and surrounding ISM (Saikia & Gupta 2003b). Also, the impact of supersonic jets onto the ISM/IGM can create cocoons of (shocked) gas and synchrotron emission with ‘hot-spot’ morphologies, while entrainment of gas by slower jets can lead to bright radio sources with edge-darkened lobes (see e.g. reviews by Bridle & Perley 1984; Ferrari 1998; Bicknell & Sutherland 2006). These external factors may thus contribute to the classical dichotomy in radio sources between Fanaroff & Riley type-I (FR-I; Fanaroff & Riley 1974) objects, with low-power, sub-relativistic jets that have an edge-darkened morphology, and type-II (FR-II) sources, with powerful, relativistic jets ending in a bright hot-spot (see e.g. Gopal-Krishna & Wiita 2000).

A particularly interesting object in this respect is the nearby ($z = 0.0115$) radio galaxy NGC 3801. NGC 3801 is classified as an FR-I radio galaxy, based on its total radio power ($P_{1.4\text{GHz}} = 2.9 \times 10^{23} \text{ W Hz}^{-1}$; Condon & Broderick 1988), radio source morphology (Jenkins 1982; Croston et al. 2007) and weak emission-line spectrum (Heckman et al. 1986). The radio source of NGC 3801 is small (~ 11 kpc; Jenkins 1982) and contained well within the optical boundaries of a peculiar early-type host galaxy, with a patchy dust feature along the major stellar axis and a perpendicular prominent inner dust-lane (Heckman et al. 1986; Verdoes Kleijn et al. 1999), as well as a distorted and box-shaped faint outer envelope (Heckman et al. 1986). The inner dust-lane coincides with a kpc-scale CO disc, oriented perpendicular to the radio axis (Das et al. 2005, see also Ocaña Flaquer et al. 2010).

X-ray observations by Croston et al. (2007) showed evidence for shocked X-ray gas in the central region of NGC 3801, created by supersonic, over-pressured jets that are not in equilibrium with the hot ISM. These X-ray studies also revealed a high absorbing column towards the nucleus of NGC 3801, likely due to an obscuring torus (Croston et al. 2007). In addition, single-dish observations showed that NGC 3801 is rich in neutral hydrogen (HI) gas (Heckman et al. 1983; Duprie & Schneider 1996). Based on its cold gas content and peculiar optical host galaxy morphology, it has been suggested that NGC 3801 could have been involved in a gas-rich galaxy-galaxy merger (Das et al. 2005; Croston et al. 2007). As speculated by Croston et al. (2007), these are all properties that are generally not associated with FR-I sources, but are believed

to be common among more powerful, high-excitation radio-loud AGN (see also Heckman et al. 1986, Baum et al. 1992, Hardcastle, Evans, & Croston 2006, Croston et al. 2008, as well as Sect. 4.4.1).

In this paper we present radio synthesis observations of the HI gas in NGC 3801. Our observations reveal that the HI gas is distributed in a large-scale disc of cold gas. The large-scale HI disc is aligned with the radio axis, indicating that the radio jets propagate directly into the cold gas disc. Based on our HI results, we discuss the formation history of NGC 3801 and investigate further how unique NGC 3801 is compared to other nearby FR-I radio galaxies.

Throughout this paper we assume $H_0 = 71 \text{ km s}^{-1} \text{ Mpc}^{-1}$, which puts NGC 3801 at a distance of 48.6 Mpc and $1 \text{ arcsec} = 0.24 \text{ kpc}$.

2 OBSERVATIONS

HI observations of NGC 3801 were performed with the Westerbork Synthesis Radio Telescope (WSRT) on 13 July 2009 during a single 12h track. A standard calibration was applied, using 3C 147 as primary calibrator. Data were reduced and analysed using the MIRIAD and KARMA software. After calibration, the continuum (‘channel-0’) data were separated from the line data by fitting a straight line to the line-free channels. A radio continuum map with uniform weighting and beam-size $10.57'' \times 37.55''$ (PA -0.4°) was produced by Fourier transforming the channel-0 data and subsequently cleaning the signal. In the same way, an HI cube with robust weighting +1 (Briggs 1995), beam-size of $22.47'' \times 87.52''$ (PA 0.2°) and channel separation of 4.1 km s^{-1} was created from the line-data.¹ We subsequently Hanning smoothed the line-data to an effective velocity resolution of $\sim 8 \text{ km s}^{-1}$, resulting in a noise level of $0.7 \text{ mJy bm}^{-1} \text{ chan}^{-1}$. Total intensity images of the HI emission were made by using a mask (derived by smoothing the positive signal both spatially and kinematically) to extract the HI line emission from the original line data-set. The data in this paper are corrected for primary beam attenuation and presented in optical barycentric velocity definition.

3 RESULTS

3.1 HI emission in NGC 3801/3802

Figure 1 show the large-scale HI disc of NGC 3801, which has a diameter of 34 kpc. A small fraction of the HI emission-line gas in the disc was detected with VLA observations by Hota et al. (2009). We derive a total mass of the emission-line gas of $M_{\text{HI}} = 1.3 \times 10^9 M_\odot$, though we note that part of the HI disc in our WSRT observations is detected in absorption against the radio continuum source (see Fig. 3) and not taken into account in this HI mass estimate. The HI emission-line gas is aligned with the host galaxy’s main stellar axis and the east-west dust-lane. The HI disc shows

¹ The large difference in beam-size between north-south and east-west direction is a result of the relatively low elevation of the source throughout the observations with the east-west array-configuration of the WSRT.

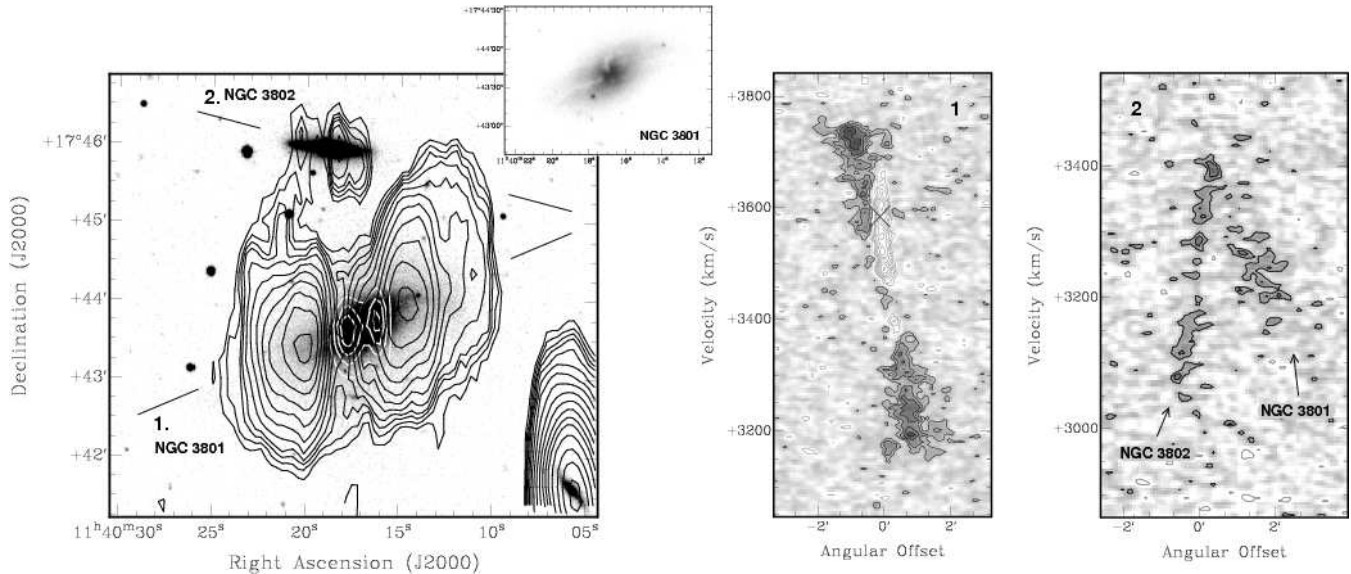


Figure 1. NGC 3801 and NGC 3802. *Left:* Total intensity of HI emission (black contours) and 1.4 GHz radio continuum (white contours) overlaid into an optical SDSS image of NGC 3801 (see also top-right inset) and NGC 3802. Note that the spatial resolution of the radio data in north-south direction is a factor of 4 worse than in east-west direction due to the highly elongated beam (Sect. 2). For clarity, HI absorption has been omitted from this plot. Contour levels HI: 0.15, 0.21, 0.28, 0.34, 0.45, 0.62, 0.84, 1.1, 1.5, 2.0, 2.5, 3.1, 3.8, 4.5, 5.2, 6.0, 7.0, $8.0 \times 10^{20} \text{ cm}^{-2}$. Contours levels radio continuum: 0.04, 0.11, 0.18, 0.25 Jy bm^{-1} . *Right:* Position velocity maps of the HI emission (black contours) and HI absorption (grey contours) along the two lines presented in the left image. Contour levels: -9.0, -7.2, -5.6, -4.2, -3.0, -2.0, -1.2 (grey), 1.2, 2.0, 3.0, 4.2 (black) mJy bm^{-1} . The cross represents the peak of CO emission from ‘clump C’ found by Das et al. (2005) (see Sect. 4.1).

regular rotation with a large velocity spread of $\Delta v \approx 600 \text{ km s}^{-1}$, corresponding to a maximum rotational velocity of $\sim 300 \text{ km s}^{-1}$ (which is larger than the rotational velocity of the optical emission-line gas; Heckman et al. 1983, 1985b). The HI disc is centred on $v_{\text{sys}} = 3452 \pm 20 \text{ km s}^{-1}$ ($z = 0.01151 \pm 0.00007$), which we argue reflects the systemic velocity of NGC 3801. Despite the regular rotation, Fig. 2 shows that the HI disc is not (yet) fully settled. The most prominent asymmetry in the HI distribution occurs at the north-western edge of the disc, with gas apparently stretching in the direction of the close gas-rich companion NGC 3802.

The close companion NGC 3802 is a disc-galaxy (S0 or spiral) approximately 33 kpc north of NGC 3801. NGC 3802 contains $M_{\text{HI}} \approx 3.9 \times 10^7 M_{\odot}$ of HI gas. The HI gas has an asymmetric distribution across NGC 3802, peaking in the western part of the disc and continuing on the eastern side, covering a total velocity range of $\sim 400 \text{ km s}^{-1}$ (see Fig. 1 - *right* for more details). While the total intensity image of Fig. 1 (*left*) shows a spurious HI bridge in between NGC 3801 and the *eastern* part of the disc of NGC 3802, we note that this is merely a projection effect. In fact, Figs. 1 (*right*) and 2 show that there is an apparent bridge or warp of HI gas stretching from the north-western part of the HI disc of NGC 3801 towards the *western* part of the disc of NGC 3802. This HI feature is too faint to be identified in the total intensity image of Fig. 1 (*left*). The asymmetric HI distribution in companion galaxy NGC 3802 and the apparent HI bridge in between NGC 3801 and NGC 3802 suggests that the NGC 3801/3802 system is in ongoing interaction.

3.2 HI absorption in NGC 3801

Figure 3 shows the HI absorption detected against the radio continuum source in the central part of NGC 3801. For the radio continuum we derive a total integrated flux of $S_{1.4 \text{ GHz}} = 1.03 \text{ Jy}$, corresponding to $P_{1.4 \text{ GHz}} = 2.9 \times 10^{23} \text{ W Hz}^{-1}$. This is in agreement with earlier results by Jenkins (1982) and Condon & Broderick (1988).

Taking into account that the HI absorption spectra shown in Fig. 3 are not entirely mutually independent, there are three distinctive features visible. These features are visualised in Fig. 4 and summarised in Table 1.

The first is a deep and narrow HI absorption at $v = 3488 \pm 20 \text{ km s}^{-1}$ ($z = 0.01163 \pm 0.00007$), which peaks at the location of the nucleus. The central velocity of this feature is in good agreement with the central velocity of $v = 3494 \pm 70 \text{ km s}^{-1}$ that Wegner et al. (2003) derive from optical spectroscopy.

The second is a broad component, covering the central region and eastern radio lobe. Figure 1 (*middle*) suggests that this broad absorption component traces HI gas as part of the large-scale HI disc, at locations where the gas is in front of the radio source.² This also means that the eastern radio jet is most likely the ‘far’ side of the radio source (where the radio continuum is behind the absorbing gas in the disc), while the western jet is the ‘near’ side.

² We note that the velocity gradient of the HI absorption as seen in Fig. 1 could be slightly steeper than that of the HI emission. This may occur because the spatial resolution of our observations is coarser than the underlying radio continuum structure, hence the HI absorption is less affected by beam-dilution than HI emission and could trace the more inner regions of the HI disc.

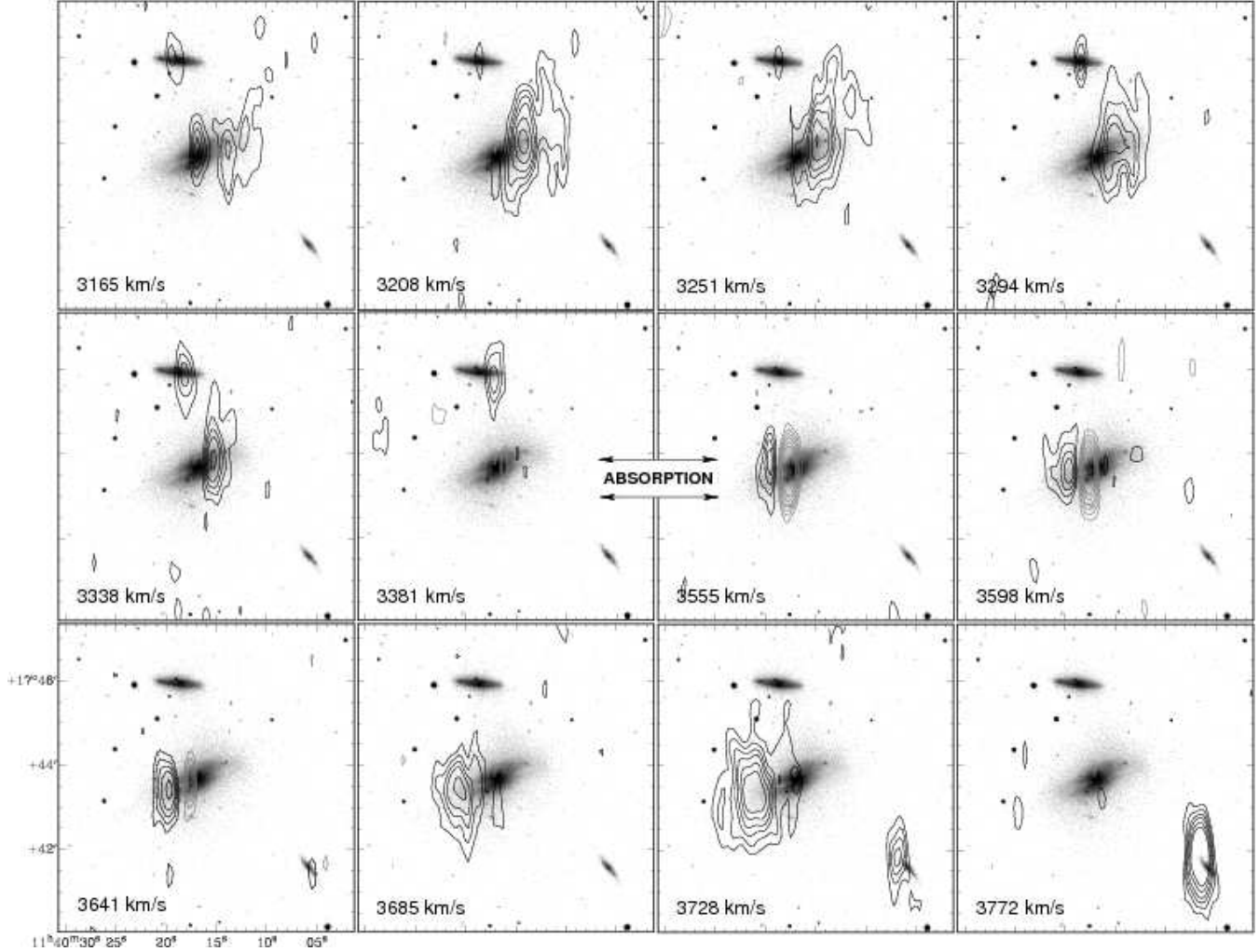


Figure 2. Channel maps of the HI emission in NGC 3801, binned to a velocity resolution of 43 km s^{-1} . The velocity range of the HI absorption is largely omitted from this plot. Contour levels: -3.2, -2.6, -2.0, -1.6, -1.2, -0.8 (grey), 0.8, 1.2, 1.6, 2.0, 2.6, 3.2 (mJy bm^{-1}).

The third feature is a narrow absorption against the western jet, which is blueshifted by $\sim 50 \text{ km s}^{-1}$ with respect to v_{sys} . Fig. 1 (*middle*) shows that also this HI component is most likely part of the large-scale, edge-on HI disc that embeds the small radio source, although it cannot be ruled out that this blueshifted HI absorption represents an outflow of neutral gas driven by the propagating radio jets. Figure 3 also shows indications of a narrow and much weaker HI absorption component against the eastern radio jet in NGC 3801, around $v \sim 3550 \text{ km s}^{-1}$.

Higher resolution HI absorption observations are essential for studying the nature of the various absorption features in more detail. For this, we refer to ongoing work by Hota et al. (2009).

3.3 HI environment

Figure 5 shows the HI environment of NGC 3801, with five other galaxies detected in HI emission. Table 2 summarises the HI properties of these systems. The bulk of the HI in

these companion galaxies is distributed in disc-like structures.

We also find two ‘clouds’ of HI gas that are not associated with an optical counterpart in the SDSS image of Fig. 5. One of them, cloud A, has a velocity that coincides with that of the eastern part of the HI disc of NGC 3801, as well as companion 3, and is located 83 kpc south of NGC 3801 (note that the velocity of cloud A is significantly offset from that of the much nearer companion 4; see Fig. 5 – *left*). Cloud B coincides in both velocity and location with the HI-rich companion 6 (NGC 3806) and is most likely gas that is either stripped off, or being accreted onto, the HI disc of NGC 3806. If these clouds of HI gas are tidal in origin, and given that the total HI mass of both clouds ($4 - 5 \times 10^7 M_{\odot}$) is similar to that of NGC 3801’s close companion NGC 3802, this indicates that past as well as ongoing interactions could have a profound influence on the evolution of this group of galaxies.

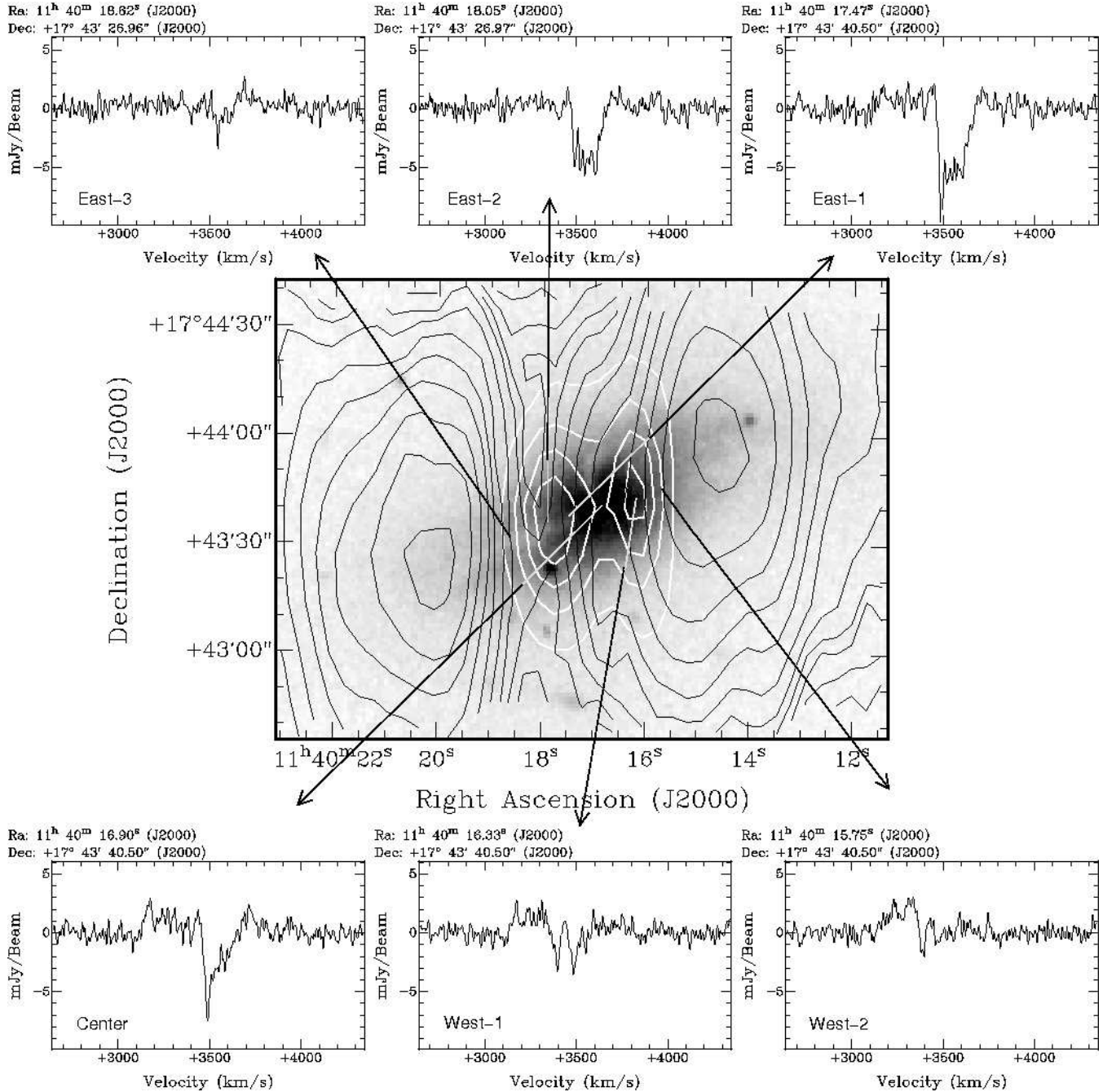


Figure 3. HI absorption properties of NGC 3801. The middle plot shows a zoom-in of the optical host galaxy, HI emission and radio continuum from Fig. 1. The zoom-windows show the HI profile at various locations along the HI disc.

4 DISCUSSION

4.1 Large-scale HI disc

Our HI results show that the bulk of the HI gas detected in earlier single-dish observations (Heckman et al. 1983; Duprie & Schneider 1996) is arranged in an HI disc with a diameter of 34 kpc, aligned along the host galaxy’s major stellar axis and prominent east-west dust-lane. We therefore argue that this large-scale HI disc traces the major axis of the host galaxy. The peak HI surface density in the disc is $\Sigma_{\text{HI}} = 2.1 M_{\odot} \text{pc}^{-2}$. This is below (or

at best close to) the critical HI surface density for star formation typically found in nearby galaxies (Kennicutt 1989; van der Hulst et al. 1993; Martin & Kennicutt 2001; Bigiel et al. 2008; Leroy et al. 2008), as also predicted by models (e.g. Schaye 2004). It is therefore unlikely that widespread star formation is happening in the disc (although star formation may occur in regions of higher local density).

The rotation of the large-scale HI disc allows us to estimate the dynamical mass of NGC 3801 to be $M_{\text{dyn}} = (Rv^2/G) \cdot \sin^{-2}i = 3.6 \times 10^{11} M_{\odot}$ (with $R=17$ kpc the radius of the HI disc, $v=300 \text{ km s}^{-1}$ its rotation velocity and assuming the HI disc is viewed edge-on, i.e. $i = 90^{\circ}$).

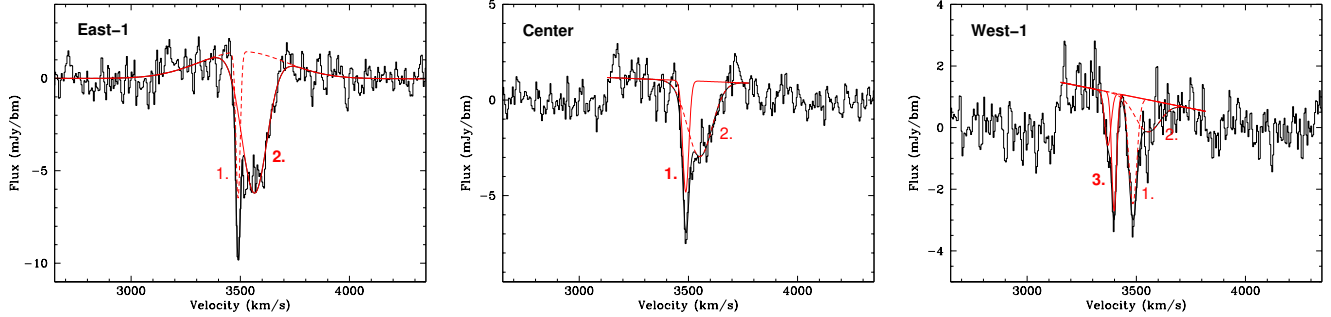


Figure 4. Gaussian fits to the HI absorption profiles of Fig. 3. The black solid line shows the total fit, while the red lines show the individual Gaussian components. The numbers correspond to the absorption features as listed in Table 1. The actual values in Table 1 are derived from the Gaussian profiles with solid red lines and thick numbers in this plot.

Table 1. HI absorption properties

Feature #	v_{centre} (km s $^{-1}$)	FWHM (km s $^{-1}$)	τ	N_{HI} ($\times 10^{20}$ cm $^{-2}$)
1	3488	33	0.035	2.1
2	3564	136	0.028	7.0
3	3399	42*	0.014	1.1*

Notes – Values have been derived from the Gaussian fits to the profiles, as shown in Fig. 4. v_{centre} is the central velocity of the absorption feature (error ± 20 km s $^{-1}$); FWHM is the full width at half the maximum intensity; τ is the maximum optical depth that the feature displays across the radio continuum and is calculated through $e^{-\tau} = 1 - \frac{S_{\text{abs}}}{S_{\text{cont}}}$ (with S_{cont} the underlying 21cm radio continuum flux at the limit spatial resolution of our observations); N_{HI} is the derived HI column density (assuming $T_{\text{spin}} = 100$ K).

*derived from both Gaussian components that comprise feature 3 in Fig. 4.

Given that $L_B = 2.3 \times 10^{10} L_{\odot}$ (Heckman, Carty, & Bothun 1985a, corrected for $H_0 = 71$ km s $^{-1}$ Mpc $^{-1}$), NGC 3801 has $M_{\text{dyn}}/L_B \approx 15$, which indicates that NGC 3801 contains a significant dark-matter halo (in agreement with M/L ratios observed in other HI-rich early-type galaxies; Bertola et al. 1993, Franx, van Gorkom, & de Zeeuw 1994, Morganti et al. 1997, Weijmans et al. 2008). Considering only the HI emission, we find $M_{\text{HI}}/L_B = 0.06$ for NGC 3801,³ which is within the range of values observed for other HI-rich early-type galaxies (Oosterloo et al. 2007, 2010) and polar-ring galaxies (Bettoni et al. 2001).

The radio source is aligned roughly along the major axis of the HI disc, indicating that the radio jets are propagating directly into the disc. Perpendicular to the large-scale HI disc and radio axis, Das et al. (2005) detected a 4.6 kpc wide CO disc, which follows a prominent inner dust-lane (Verdoes Kleijn et al. 1999). We refer to Das et al. (2005, their figure 5) for an excellent illustrative image of the inner region of NGC 3801 (which shows contour plots of the CO(1-0) and VLA 20cm radio continuum overlaid onto an HST image of the inner dust features).

³ Note that this estimate does not take into account the HI gas detected in absorption, therefore the true value of M_{HI}/L_B is somewhat larger.

Das et al. (2005) also detected a CO clump that is not part of the inner CO disc and aligned along the EW dust-lane, with a projected distance of about 2 kpc from the nucleus. They dismiss the likelihood that this CO clump is part of a second disc, given that it would require the geometry of the inner and outer disc to be extremely rare (roughly one in a thousand), namely such that both discs would have to be edge-on, within 10° of the line-of-sight and perpendicular to each other to within 10° . Our HI results, however, show that NGC 3801 does in fact satisfy the conditions of two perpendicular, edge-on discs (an inner kpc-scale CO disc and a large-scale outer HI disc). Figure 1 shows that the CO clump detected by Das et al. (2005) likely represents cold molecular gas that is part of the large-scale outer disc. Given that two discs with intersecting orbits are not stable, it is likely that the large-scale HI disc has a central gap and thus may not continue all the way down to the kpc-scale central region.

Our HI results (Fig. 1 – *middle* and Fig. 2), however, show that there is neutral gas in the central region, which has a steep velocity gradient relative to the bulk of the gas in the large-scale HI disc. This HI component is most clear in Fig. 2 at $v = 3165$ km s $^{-1}$ (panel 1), $v = 3251$ km s $^{-1}$ (panel 3) and $v = 3728$ km s $^{-1}$ (panel 11), of which the latter two correspond to the velocity of the two clumps of CO gas that represent the central molecular disk in Das et al. (2005). This could indicate an HI counterpart to the central CO disc, although the spatial resolution of our HI observations is too poor to verify this.

From an HI perspective, NGC 3801 is not unique. Similar to NGC 3801, examples of other early-type systems with a perpendicular inner and outer disc are known to exist, possibly related to the tri-axial nature of the mass distribution. These include NGC 5266 (Morganti et al. 1997) and NGC 2685 (where the two discs/rings are likely a projection effect of an extremely warped disc; Józsa et al. 2009). NGC 3801 also bears resemblance to polar-ring galaxies, such as NGC4650A (Arnaboldi et al. 1997) and UGC 9796 (Cox, Sparke, & van Moorsel 2006).

4.2 Formation history and AGN triggering

Based on its peculiar optical morphology and CO content in the inner few kpc, it has been suggested that NGC 3801 could have been involved in a gas-rich galaxy-galaxy merger

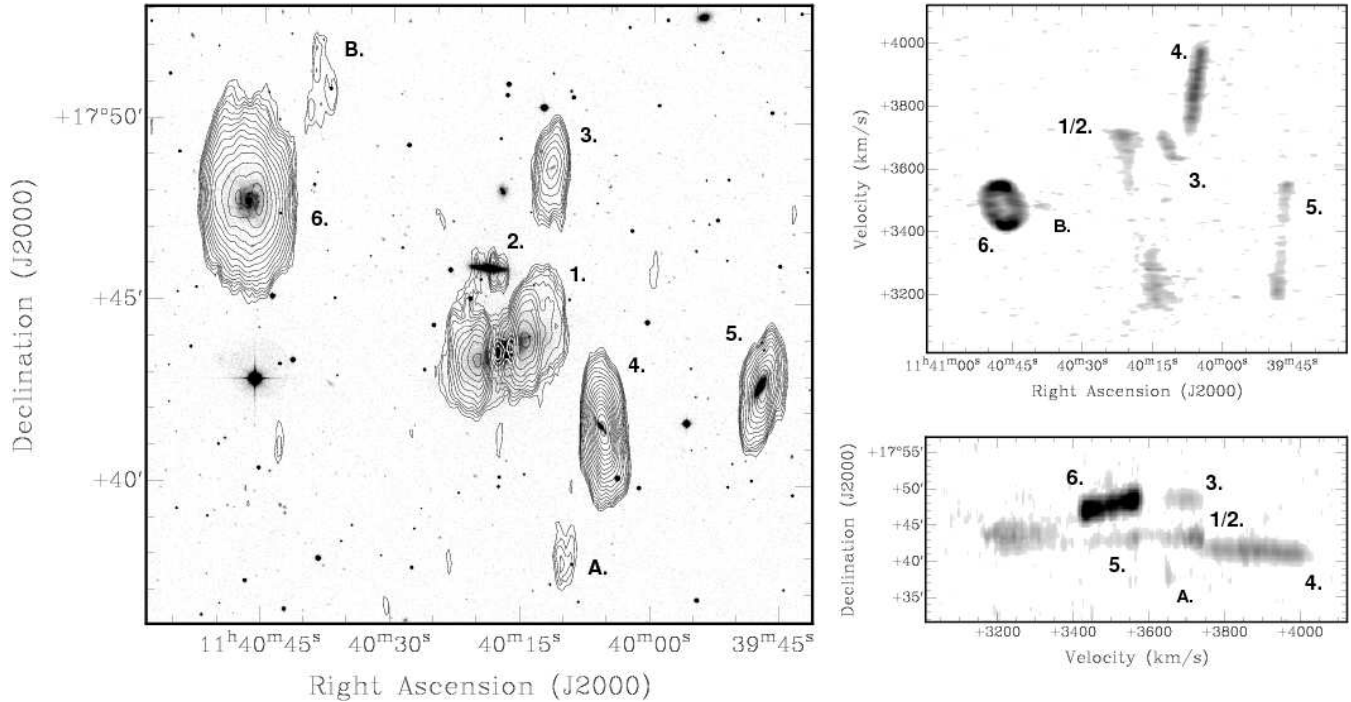


Figure 5. HI environment of NGC 3801. *Left:* Contours of the total intensity HI emission (black) overlaid onto an optical SDSS image. Contour levels HI: 0.15, 0.21, 0.28, 0.34, 0.45, 0.62, 0.84, 1.1, 1.5, 2.0, 2.5, 3.1, 3.8, 4.5, 5.2, 6.0, 7.0, $8.0 \times 10^{20} \text{ cm}^{-2}$. The 1.4 GHz radio continuum source is represented by white contours in the very central region of NGC 3801 (levels: 0.04, 0.11, 0.18, 0.25 Jy bm^{-1}). For clarity, HI absorption has been omitted from this plot. *Right:* Position-velocity plots of the same HI data cube, represented as total intensity of the HI emission integrated along the RA and dec axes.

Table 2. HI companions

#	Name	D (kpc)	v_{sys} (km s ⁻¹)	Δv	M_{HI} (M_{\odot})
1	NGC 3801	-	3552 ± 20	607	1.3×10^9
2	NGC 3802	33	3250 ± 40	398	3.9×10^7
3	J114011.27+174846.6	75	3674 ± 20	103	3.1×10^8
4	KUG 1137+179	49	3858 ± 40	308	2.0×10^9
5	NGC 3790	102	3373 ± 40	380	6.3×10^8
6	NGC 3806	118	3486 ± 20	180	4.0×10^9
	'Cloud A'	83	3657 ± 20	-	3.8×10^7
	'Cloud B'	132	3496 ± 20	-	5.0×10^7

Notes – D is the projected distance to NGC 3801; v_{sys} is the central optical barycentric velocity derived from our HI data; Δv is the velocity range covered by the HI emission; M_{HI} is the total HI mass detected in emission.

(e.g. Heckman et al. 1986; Das et al. 2005; Croston et al. 2007). Our HI results are in agreement with such a scenario, given that the formation of a large-scale HI disc can be the natural outcome of a galaxy merger over significant time-scales (e.g. Emonts et al. 2006, 2008; Serra et al. 2006). Simulations of merging galaxies by Di Matteo et al. (2007) show that gaseous and stellar discs in the progenitor galaxies can be tidally disrupted, depending on the orbital parameters of the merging galaxies (in particular direct encounters can create large gaseous tidal-tails). Barnes (2002) shows that part of this expelled material can be re-accreted back onto the newly formed host galaxy and settle into a large-scale gas disc on time-scales of one to several Gyr. The bulk of the HI gas in the disc of NGC 3801 shows regular rotation, which means that the gas must have had enough time to settle into the observed disc-like structure. As a rough es-

timate of the merger time-scale, we assume that this process must have lasted at least one orbital period, or $\geq 3.5 \times 10^8$ yr.

The age of the radio source is significantly less than this ($\leq 2.4 \times 10^6$ yr; Croston et al. 2007). While there is no evidence for a direct causal connection between the possible merger event and the triggering of the radio source, there would have been a significant time-delay between the start of the merger and the onset of the current episode of the radio-AGN activity. Similar time-delays between merger (and associated starburst episode) and radio-AGN activity have been observed in other nearby radio galaxies (e.g. Evans et al. 1999; Tadhunter et al. 2005; Emonts et al. 2006, 2008; Labiano et al. 2008).

We note, however, that our HI results alone do not provide conclusive evidence that the large-scale HI disc in

NGC 3801 was formed as a result of a major merger. Minor mergers or interactions with satellite galaxies (similar to the ongoing interaction between NGC 3801 and NGC 3802) may also have played a role in both shaping the HI disc as well as triggering nuclear activity in NGC 3801. Given that the bulk of the HI gas that we find in our data cube is associated with companion galaxies that are all within $v \sim 300$ km s⁻¹ from the central velocity of NGC 3801, it is possible that the HI gas in the disc of NGC 3801 was delivered by former gas-rich companions over the course of several Gyr (similar to what is discussed by Struve et al. 2010a for the large HI disc in radio galaxy NGC 1167).

Another possibility is that accretion of cold gas played a major role in the formation of the HI disc. Simulations by Macciò et al. (2006) show that extended rings of gas in polar-ring galaxies may form naturally through the accretion of cold gas falling in along large filamentary structures, while Bournaud & Combes (2003) argue that it is more likely for polar-ring galaxies to acquire their gaseous discs through tidal accretion from a gas-rich donor galaxy rather than a violent merger. A similar mechanism may have formed the large-scale HI disc in NGC 3801.

4.3 Radio source evolution

As mentioned above, the alignment of the small radio source in NGC 3801 with the large-scale outer HI disc makes NGC 3801 an ideal nearby radio galaxy for studying the early stage of radio-source evolution and its interaction with the surrounding cold ISM.

Croston et al. (2007) find evidence for shocked heated shells of hot gas associated with the radio source in NGC 3801, caused by supersonic, over-pressured radio jets. Their findings indicate that the radio source in NGC 3801 is heavily interacting with the surrounding ISM. In proceedings based on high-resolution VLA HI observations, Hota et al. (2009) report the presence of a broad, faint, blueshifted absorption and an HI clump associated with the shocked shell around the eastern lobe, possibly reflecting a gas outflow. Our lower resolution HI data do not show clear evidence for a broad, blueshifted absorption, but such a faint HI absorption feature could be filled in with HI emission within the relatively large beam of our observations. We do detect an apparent blueshifted narrow absorption component against the western radio lobe, but as discussed in Sect. 3.2, this most likely represents HI gas as part of the large-scale HI disc.

Similar to NGC 3801, there are other known radio galaxies in which the radio source propagates into an outer HI disc. This includes Coma A, where the radio lobes ionise part of the disc (Morganti et al. 2002) and IC 5063, where the radio jets produce fast outflows of HI gas (Morganti et al. 1998; Oosterloo et al. 2000). Particularly interesting is also the similarity with the disc-dominated radio galaxy B2 0722+30, which hosts a small FR-I radio source (similar to NGC 3801) that propagates close to the plane of the disc, in the direction of a heavily interacting HI-rich galaxy pair (Emons et al. 2009).

4.4 HI-rich radio galaxies: the general picture

In general, roughly 10% of early-type galaxies outside clusters contain large amounts of HI gas ($M_{\text{HI}} \geq 10^9 M_{\odot}$), often distributed in large-scale disc- or ring-like structures (Sadler 2001; Morganti et al. 2006; Oosterloo et al. 2007, 2010).⁴ In Emons et al. (2010), we showed that the overall HI properties of nearby, non-cluster low-power radio galaxies are similar to those of radio-quiet early-type galaxies, with large-scale HI discs detected in a significant fraction of radio-loud systems. In addition, we showed that there is a clear segregation in HI content with radio size, in the sense that massive, large-scale HI discs are only found in the host galaxies of compact radio sources, while none of the more extended FR-I radio sources studied contain similar amounts of HI gas (Emons et al. 2007, 2010). The radio source in NGC 3801 is ~ 11 kpc in diameter (Jenkins 1982). As illustrated in Fig. 6, the HI properties of NGC 3801 are thus similar to those of a significant fraction of nearby low-power compact radio sources.

It is likely that in these systems the early evolution of the radio source is intimately linked with the surrounding cold ISM, and that either confinement by the dense ISM or inefficient fuelling (through clumpiness of the cold ISM and associated non-steady accretion) keeps the radio source compact (see discussions in Emons et al. 2007, 2010). An alternative scenario, recently raised by Morganti et al. (2011) in a study of the powerful compact radio source PKS 1814-637, suggests that the radio emission in these HI-rich compact radio sources may be boosted, at least temporarily, by the interaction of the radio jets with the rich ISM, implying that intrinsically these compact sources may reflect a link to radio-AGN in Seyfert galaxies (see also Emons et al. 2010, where we speculate that the transition from radio-AGN in Seyferts to the brighter compact radio sources to classical FR-Is may perhaps be linked to a transition from well-defined star-forming HI discs to low surface brightness HI discs to HI-poor host galaxies).

4.4.1 NGC 3801: a classical FR-I?

NGC 3801 is classified as an FR-I radio galaxy, based on its total radio power ($P_{1.4\text{GHz}} = 2.9 \times 10^{23}$ W Hz⁻¹), radio source morphology (Jenkins 1982; Croston et al. 2007) and weak emission-line spectrum (Heckman et al. 1986). However, X-ray observations by Croston et al. (2007) show that NGC 3801 has supersonic, over-pressured radio jets, not commonly found in FR-I sources (Croston et al. 2008). These X-ray studies also reveal a high absorbing column towards the nucleus (possibly representing an obscuring torus), something that is generally not associated with FR-I sources (Hardcastle et al. 2006; Croston et al. 2007). Croston et al. (2007) suggest that these properties may more closely resemble those of high-power, high-excitation FR-II sources, which are believed to be post-merger systems that are fuelled by cold gas driven into the central region to form a radiatively-efficient classical accretion disc (contrary to low-power/low-excitation FR-Is, which are believed to be

⁴ di Serego Alighieri et al. (2007) and Oosterloo et al. (2010) show that the HI detection rate of early-type galaxies in the Virgo Cluster is dramatically lower.

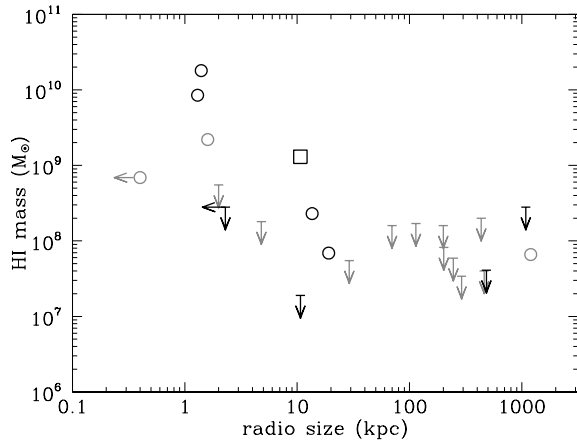


Figure 6. Adapted from Emonts et al. (2010). Shown is the HI mass content (or upper limit) plotted against the total linear extent of the radio source for a complete sample of nearby non-cluster, low-power (FR-I-type) radio galaxies. The square represents NGC 3801. See Emonts et al. (2007) and Emonts et al. (2010) for details. For completeness, radio host galaxies designated as elliptical (E) in the NASA Extra-galactic Database (NED) are plotted in grey, while non-ellipticals (S0 and merger systems) are black. While this reflects the long known idea that the relative HI fraction seems to rise from ellipticals to S0 and later-type systems (e.g. Wardle & Knapp 1986), it also shows that the HI-rich compact radio sources in this sample are hosted by galaxies with a variety of optical morphologies (see Emonts et al. 2010, for detailed optical imaging).

fuelled mainly through a quasi-spherical Bondi accretion of circum-galactic hot gas directly onto the nucleus; see e.g. Heckman et al. 1986, Baum et al. 1992, Hardcastle et al. 2006, Hardcastle, Evans, & Croston 2007, Baldi & Capetti 2008, Emonts et al. 2010, Ramos Almeida et al. 2011). This scenario is in agreement with our HI results, which show that NGC 3801 is likely a post-merger system with large amounts of cold gas.⁵

However, as we saw in Sect. 4.4, the presence of a large-scale HI disc is not unusual for low-power compact radio sources like NGC 3801. We speculate that the possible link to radio-loud Seyferts (discussed in Sect. 4.4) could perhaps also explain some of the unusual characteristics of NGC 3801. Many Seyfert-AGN also show heavy obscuration in X-rays (e.g. Maiolino et al. 1998, Risaliti, Maiolino, & Salvati 1999, Cappi et al. 2006) and can be found in disc-dominated, interacting galaxies that contain large amounts of HI gas (e.g. Kuo et al. 2008).

Regardless of the exact nature of the radio-loud AGN, the combined X-ray and HI results suggests that NGC 3801 is a system with over-pressured radio jets that are embedded in (and interacting with) a rich, ambient cold ISM that has been deposited after a gas-rich merger; features not or no longer present in more evolved FR-I radio sources. As discussed by Croston et al. (2007), this resembles the case of

⁵ Our HI results do not show evidence that cold gas is being accreted onto the central region (see Section 3.2), but note that the accretion rate necessary to sustain AGN activity could be so low that it is well beyond our observing capabilities (van Gorkom et al. 1989).

Centaurus A (see also Kraft et al. 2003; van Gorkom et al. 1990; Schiminovich et al. 1994; Struve et al. 2010b). X-ray observations of other HI-rich compact FR-I radio sources may reveal how unique NGC 3801 (and Cen A) are in the evolution of classical radio sources.

5 CONCLUSIONS

We have shown that the HI gas in NGC 3801 – detected in earlier single-dish observations by Heckman et al. (1983) and Duprie & Schneider (1996) – is distributed in a regularly rotating large-scale HI disc. We also detect HI gas in the close companion NGC 3802 (which is in apparent ongoing interaction with NGC 3801) as well as several other galaxies and gas clouds in the immediate environment of NGC 3801. The small radio source in NGC 3801 is propagating directly into the large-scale HI disc, making NGC 3801 an important system for investigating in detail the evolution of a small radio source through its host galaxy’s cold ISM. Because of the similarity between the HI properties of NGC 3801 and those of other nearby low-power compact radio sources, studying NGC 3801 may reveal important insight into the early evolution of at least a significant fraction of low-power radio sources.

ACKNOWLEDGMENTS

We thank the referee Dhruba Saikia for suggestions that significantly improved this paper. The Westerbork Synthesis Radio Telescope is operated by the ASTRON (Netherlands Institute for Radio Astronomy) with support from the Netherlands Foundation for Scientific Research (NWO).

REFERENCES

- Alexander D. M., Smail I., Bauer F. E., Chapman S. C., Blain A. W., Brandt W. N., Ivison R. J., 2005, *Nature*, 434, 738
- Arnaboldi M., Oosterloo T., Combes F., Freeman K. C., Koribalski B., 1997, *AJ*, 113, 585
- Baldi R. D., Capetti A., 2008, *A&A*, 489, 989
- Barnes J. E., 2002, *MNRAS*, 333, 481
- Baum S. A., Heckman T. M., van Breugel W., 1992, *ApJ*, 389, 208
- Bertola F., Pizzella A., Persic M., Salucci P., 1993, *ApJL*, 416, L45
- Bettoni D., Galletta G., García-Burillo S., Rodríguez-Franco A., 2001, *A&A*, 374, 421
- Bicknell G. V., Sutherland R. S., 2006, *AN*, 327, 235
- Bicknell G. V., Sutherland R. S., van Breugel W. J. M., Dopita M. A., Dey A., Miley G. K., 2000, *ApJ*, 540, 678
- Bigiel F., Leroy A., Walter F., Brinks E., de Blok W. J. G., Madore B., Thornley M. D., 2008, *AJ*, 136, 2846
- Bournaud F., Combes F., 2003, *A&A*, 401, 817
- Bridle A. H., Perley R. A., 1984, *ARA&A*, 22, 319
- Briggs D. S., 1995, PhD thesis, New Mexico Institute of Mining and Technology
- Cappi M. et al., 2006, *A&A*, 446, 459
- Chambers K. C., Miley G. K., van Breugel W., 1987, *Nature*, 329, 604

- Clark N. E., Axon D. J., Tadhunter C. N., Robinson A., O'Brien P., 1998, *ApJ*, 494, 546
- Condon J. J., Broderick J. J., 1988, *AJ*, 96, 30
- Cox A. L., Sparke L. S., van Moorsel G., 2006, *AJ*, 131, 828
- Croston J. H., Kraft R. P., Hardcastle M. J., 2007, *ApJ*, 660, 191
- Croston J. H., Hardcastle M. J., Birkinshaw M., Worrall D. M., Laing R. A., 2008, *MNRAS*, 386, 1709
- Das M., Vogel S. N., Verdoes Kleijn G. A., O'Dea C. P., Baum S. A., 2005, *ApJ*, 629, 757
- Di Matteo T., Springel V., Hernquist L., 2005, *Nature*, 433, 604
- Di Matteo P., Combes F., Melchior A.-L., Semelin B., 2007, *A&A*, 468, 61
- di Serego Alighieri S. et al., 2007, *A&A*, 474, 851
- Duprie K., Schneider S. E., 1996, *AJ*, 112, 937
- Emons B. H. C., Morganti R., Tadhunter C. N., Oosterloo T. A., Holt J., van der Hulst J. M., 2005, *MNRAS*, 362, 931
- Emons B. H. C., Morganti R., Tadhunter C. N., Holt J., Oosterloo T. A., van der Hulst J. M., Wills K. A., 2006, *A&A*, 454, 125
- Emons B. H. C., Morganti R., Oosterloo T. A., van der Hulst J. M., van Moorsel G., Tadhunter C. N., 2007, *A&A*, 464, L1
- Emons B. H. C., Morganti R., van Gorkom J. H., Oosterloo T. A., Brogt E., Tadhunter C. N., 2008, *A&A*, 488, 519
- Emons B. H. C., Tadhunter C. N., Morganti R., Oosterloo T. A., Holt J., Brogt E., van Moorsel G., 2009, *MNRAS*, 396, 1522
- Emons B. H. C. et al., 2010, *MNRAS*, 406, 987
- Evans A. S., Kim D. C., Mazzarella J. M., Scoville N. Z., Sanders D. B., 1999, *ApJL*, 521, L107
- Fanaroff B. L., Riley J. M., 1974, *MNRAS*, 167, 31P
- Ferrarese L., Merritt D., 2000, *ApJL*, 539, L9
- Ferrari A., 1998, *ARA&A*, 36, 539
- Franx M., van Gorkom J. H., de Zeeuw T., 1994, *ApJ*, 436, 642
- Gopal-Krishna, Wiita P. J., 2000, *A&A*, 363, 507
- Guillard P. et al., 2011, *ApJ* (in prep.)
- Hardcastle M. J., Evans D. A., Croston J. H., 2006, *MNRAS*, 370, 1893
- , 2007, *MNRAS*, 376, 1849
- Heckman T. M., Balick B., van Breugel W. J. W., Miley G. K., 1983, *AJ*, 88, 583
- Heckman T. M., Carty T. J., Bothun G. D., 1985a, *ApJ*, 288, 122
- Heckman T. M., Illingworth G. D., Miley G. K., van Breugel W. J. M., 1985b, *ApJ*, 299, 41
- Heckman T. M., Smith E. P., Baum S. A., van Breugel W. J. M., Miley G. K., Illingworth G. D., Bothun G. D., Balick B., 1986, *ApJ*, 311, 526
- Holt J., Tadhunter C., Morganti R., Bellamy M., González Delgado R. M., Tzioumis A., Inskip K. J., 2006, *MNRAS*, 370, 1633
- Holt J., Tadhunter C. N., Morganti R., 2008, *MNRAS*, 387, 639
- Holt J., Tadhunter C. N., Morganti R., Emons B. H. C., 2011, *MNRAS*, 410, 1527
- Hopkins P. F., Hernquist L., Cox T. J., Di Matteo T., Martini P., Robertson B., Springel V., 2005, *ApJ*, 630, 705
- Hota A., Lim J., Ohya Y., Saikia D. J., Dihn-v-Trung, Croston J. H., 2009, in *Astronomical Society of the Pacific Conference Series*, Vol. 407, *The Low-Frequency Radio Universe*, D. J. Saikia, D. A. Green, Y. Gupta, & T. Venturi, ed., p. 104
- Humphrey A., Villar-Martín M., Fosbury R., Vernet J., di Serego Alighieri S., 2006, *MNRAS*, 369, 1103
- Jenkins C. R., 1982, *MNRAS*, 200, 705
- Jeyakumar S., Wiita P. J., Saikia D. J., Hooda J. S., 2005, *A&A*, 432, 823
- Józsa G. I. G., Oosterloo T. A., Morganti R., Klein U., Erben T., 2009, *A&A*, 494, 489
- Kennicutt Jr. R. C., 1989, *ApJ*, 344, 685
- Kraft R. P., Vázquez S. E., Forman W. R., Jones C., Murray S. S., Hardcastle M. J., Worrall D. M., Churazov E., 2003, *ApJ*, 592, 129
- Kuo C.-Y., Lim J., Tang Y.-W., Ho P. T. P., 2008, *ApJ*, 679, 1047
- Labiano A., O'Dea C. P., Barthel P. D., de Vries W. H., Baum S. A., 2008, *A&A*, 477, 491
- Leroy A. K., Walter F., Brinks E., Bigiel F., de Blok W. J. G., Madore B., Thornley M. D., 2008, *AJ*, 136, 2782
- Macciò A. V., Moore B., Stadel J., 2006, *ApJL*, 636, L25
- Maiolino R., Salvati M., Bassani L., Dadina M., della Ceca R., Matt G., Risaliti G., Zamorani G., 1998, *A&A*, 338, 781
- Martin C. L., Kennicutt Jr. R. C., 2001, *ApJ*, 555, 301
- McCarthy P. J., van Breugel W., Spinrad H., Djorgovski S., 1987, *ApJL*, 321, L29
- McCarthy P. J., Baum S. A., Spinrad H., 1996, *ApJS*, 106, 281
- Morganti R., Sadler E. M., Oosterloo T., Pizzella A., Bertola F., 1997, *AJ*, 113, 937
- Morganti R., Oosterloo T., Tsvetanov Z., 1998, *AJ*, 115, 915
- Morganti R., Oosterloo T. A., Tinti S., Tadhunter C. N., Wills K. A., van Moorsel G., 2002, *A&A*, 387, 830
- Morganti R., Oosterloo T. A., Emons B. H. C., van der Hulst J. M., Tadhunter C. N., 2003, *ApJL*, 593, L69
- Morganti R., Oosterloo T. A., Tadhunter C. N., van Moorsel G., Emons B., 2005a, *A&A*, 439, 521
- Morganti R., Tadhunter C. N., Oosterloo T. A., 2005b, *A&A*, 444, L9
- Morganti R. et al., 2006, *MNRAS*, 371, 157
- Morganti R., Holt J., Saripalli L., Oosterloo T. A., Tadhunter C. N., 2007, *A&A*, 476, 735
- Morganti R., Holt J., Tadhunter C., Ramos Almeida C., Dicken D., Inskip K., Oosterloo T., Tzioumis T., 2011, *A&A*, 535, 97
- Ocaña Flaquer B., Leon S., Combes F., Lim J., 2010, *A&A*, 518, 9
- Oosterloo T. A., Morganti R., Tzioumis A., Reynolds J., King E., McCulloch P., Tsvetanov Z., 2000, *AJ*, 119, 2085
- Oosterloo T. A., Morganti R., Sadler E. M., van der Hulst T., Serra P., 2007, *A&A*, 465, 787
- Oosterloo T. et al., 2010, *MNRAS*, 409, 500
- Ramos Almeida C., Tadhunter C. N., Inskip K. J., Morganti R., Holt J., Dicken D., 2011, *MNRAS*, 410, 1550
- Risaliti G., Maiolino R., Salvati M., 1999, *ApJ*, 522, 157
- Sadler E. M., 2001, in *Astronomical Society of the Pacific*

- Conference Series, Vol. 240, Gas and Galaxy Evolution, J. E. Hibbard, M. Rupen, & J. H. van Gorkom, ed., p. 445
- Saikia D. J., Gupta N., 2003b, *A&A*, 405, 499
- Saikia D. J., Jeyakumar S., Wiita P. J., Sanghera H. S., Spencer R. E., *MNRAS*, 276, 1215
- Saikia D. J., Jeyakumar S., Salter C. J., Thomasson P., Spencer R. E., Mantovani F., 2001, *MNRAS*, 321, 37
- Saikia D. J., Jeyakumar S., Mantovani F., Salter C. J., Spencer R. E., Thomasson P., Wiita P. J., 2003a, *PASA*, 20, 50
- Saxton C. J., Bicknell G. V., Sutherland R. S., 2002a, *ApJ*, 579, 176
- Saxton C. J., Sutherland R. S., Bicknell G. V., Blanchet G. F., Wagner S. J., 2002b, *A&A*, 393, 765
- Schaye J., 2004, *ApJ*, 609, 667
- Schimminovich D., van Gorkom J. H., van der Hulst J. M., Kasow S., 1994, *ApJL*, 423, L101
- Serra P., Trager S. C., van der Hulst J. M., Oosterloo T. A., Morganti R., 2006, *A&A*, 453, 493
- Silk J., Rees M. J., 1998, *A&A*, 331, L1
- Springel V., Di Matteo T., Hernquist L., 2005, *MNRAS*, 361, 776
- Struve C., Oosterloo T., Sancisi R., Morganti R., Emonts B. H. C., 2010a, *A&A*, 523, 75
- Struve C., Oosterloo T. A., Morganti R., Saripalli L., 2010b, *A&A*, 515, 67
- Sutherland R. S., Bicknell G. V., 2007, *ApJS*, 173, 37
- Tadhunter C. N., 1991, *MNRAS*, 251, 46P
- Tadhunter C., Robinson T. G., González Delgado R. M., Wills K., Morganti R., 2005, *MNRAS*, 356, 480
- van der Hulst J. M., Skillman E. D., Smith T. R., Bothun G. D., McGaugh S. S., de Blok W. J. G., 1993, *AJ*, 106, 548
- van Gorkom J. H., Knapp G. R., Ekers R. D., Ekers D. D., Laing R. A., Polk K. S., 1989, *AJ*, 97, 708
- van Gorkom J. H., van der Hulst J. M., Haschick A. D., Tubbs A. D., 1990, *AJ*, 99, 1781
- Verdoes Kleijn G. A., Baum S. A., de Zeeuw P. T., O'Dea C. P., 1999, *AJ*, 118, 2592
- Villar-Martín M., Binette L., Fosbury R. A. E., 1999, *A&A*, 346, 7
- Wagner A. Y., Bicknell G. V., 2011, *ApJ*, 728, 29
- Wardle M., Knapp G. R., 1986, *AJ*, 91, 23
- Wegner G. et al., 2003, *AJ*, 126, 2268
- Weijmans A.-M., Krajnović D., van de Ven G., Oosterloo T. A., Morganti R., de Zeeuw P. T., 2008, *MNRAS*, 383, 1343